Effects of energy dissipation on anisotropic materials

Zhang Ling-Yun(张凌云)†

Beijing National Laboratory for Condensed Matter Physics, Institute of Physics, Chinese Academy of Sciences, Beijing 100190, *China*

(Received 6 January 2015; revised manuscript received 1 April 2015; published online 18 May 2015)

A model and its simulations are presented to describe the effects of energy dissipation on anisotropic systems. When the current electromigration is constant, energy dissipation depends on lattice constants, resistivity, and the angles along the longitudinal and transversal directions. It is shown that an orientation variation of the grain can significantly influence the energy dissipation for some anisotropic materials. Based on calculations for the grain model, the mechanism of grain growth and microstructure evolution under electromigration is explained. Theoretical implications about material selection and reliability are derived.

Keywords: electromigration, energy dissipation

PACS: 65.40.gh, 81.05.Bx, 66.30.Qa, 68.65.Ac **DOI:** 10.1088/1674-1056/24/7/076501

1. Introduction

The phonon vibration in the metal plays a dominant role under low current density because the scattering does not cause large displacements of the ions.[1] However, under high current density, the transport of the current can enhance the atom displacement and influence the transport of mass.[2,3] This kind of mass transport by the electric field and charge carriers is called electromigration.[4–6] The high current density will increase local temperature and produce higher Joule heating. The Joule heating causes microstructural changes of solder alloys and damages severely the solder joints.[7–12] With the miniaturization of conductors, especially nano-size and meso-size conductors, the study of anisotropic properties is very important due to the geometric characteristics of nanowires and nanotubes.[13–18] From the technological viewpoint, electromigration is a major failure in the operation of solid state electronic devices. From the theoretical viewpoint, electromigration involves microscopic electric fields and subtle dynamical processes occurring in coupled electron and atom transportation.[19] The nano-scale conductors can carry much larger current densities than their macroscopic counterparts.[20–26]

This paper aims to understand the electromigration failure mechanism in anisotropic materials. We hope to stress that the Joule heating is fairly harmful under high current density and will adopt the energy dissipation to replace the Joule heating since two concepts are equivalent based on energy conservation. Synchrotron radiation white beam x-ray micro diffraction was used to follow grain-by-grain changes in the thin film Sn strips under electromigration, and grain growth and grain rotation are obtained.[27–29] We will construct a few structural models to demonstrate the important role of the anisotropic properties in the microstructure evolution under electromigration.

This paper is organized as follows. In Section 2, a general formula for calculating the energy dissipation is established. The formula of an isotropic system is obtained. We derive the expression of energy dissipation for anisotropic structure under the condition of constant current, and find that the energy dissipation depends on the lattice constants and the resistivity. The relationship between the energy dissipation and the angles along the longitudinal and transverse directions is also described. In Section 3, results and a discussion are given. We calculate the energy dissipation of two specific cases: the sandwich structure and the multilayer structure with repeatable AB stack. Numerical simulations show that the orientation variation of grain can significantly influence the energy dissipation for some anisotropic materials.

2. Theory

To describe the effect of energy dissipation on anisotropic materials, the isotropic, anisotropic, and rotating anisotropic geometric bodies are investigated by applying the condition of the constant electric current to link these different models. The relationship between the electric field and electric current can be written as

$$\boldsymbol{j} = \overleftrightarrow{\boldsymbol{\Sigma}} \cdot \boldsymbol{E}, \tag{1}$$

where $\boldsymbol{j} = \{j_x, j_y, j_z\}$ is the electric current density, $\boldsymbol{E} = \{E_x, E_y, E_z\}$ is the electric field, and $\overleftrightarrow{\boldsymbol{\Sigma}}$ stands for the electrical conductivity that reflects the physics properties of materials.[30,31] Its tensor form is

$$\overleftrightarrow{\boldsymbol{\Sigma}} = \begin{pmatrix} \sigma_{xx} & \sigma_{xy} & \sigma_{xz} \\ \sigma_{yx} & \sigma_{yy} & \sigma_{yz} \\ \sigma_{zx} & \sigma_{zy} & \sigma_{zz} \end{pmatrix}. \tag{2}$$

The expression of electric current that goes through the

†Corresponding author. E-mail: lyzhang@iphy.ac.cn

© 2015 Chinese Physical Society and IOP Publishing Ltd

cross section for any geometric structure is

$$I = \int \boldsymbol{j} \cdot \mathrm{d}\boldsymbol{S}. \tag{3}$$

On the other hand, the average electric power can be defined as

$$\overline{P} = \frac{1}{V} \iiint \boldsymbol{E} \cdot [\overleftrightarrow{\boldsymbol{\Sigma}} \cdot \boldsymbol{E}] \mathrm{d}V, \tag{4}$$

which is a scalar that represents the energy dissipation.

Based on these first principle formulae, we compare the different characteristics between the isotropic structure and the anisotropic structure. l_x, l_y, and l_z are the lattice constants along the x, y, and z directions respectively, and a, b, and c are the lattice lengths along the x axis, y axis, and z axis respectively. Therefore, $a = n_x l_x$, $b = n_y l_y$, and $c = n_z l_z$ where n_x, n_y, and n_z are the numbers of lattice sites in the x, y, and z directions.

In the isotropic geometric structure, the grain with the cubic body includes many unit cells. These unit cells are assumed to have the same size. In this case, the physical quantities in the three axes have the same value. Therefore, the electric current and the electric power can be obtained respectively, $I_i = 3\sigma_0 E_0 ab$ and $\overline{P_i} = 3\sigma_0 \overline{E_0^2}$. One of the simplest anisotropic structures is a tetragonal structure, $a = b \neq c$. In the anisotropic case, the elements of conductivity are $\sigma_{xx} = \sigma_{yy} = \sigma_0$ and $\sigma_{zz} = \sigma_z$, the other elements are zero. The x and y components of the electric field are $E_x = E_y = E_0$, but the z component of electric field E_z is a different value. Therefore, we can give the expression of the electric current

$$I_\mathrm{a} = \sigma_0 E_0 (a+b)c + \sigma_z E_z ab, \tag{5}$$

and the average electric power is

$$\overline{P_\mathrm{a}} = 2\sigma_0 \overline{E_0^2} + \sigma_z \overline{E_z^2}. \tag{6}$$

If the electric current keeps the same value both in isotropic and anisotropic cases, i.e., $I_\mathrm{i} = I_\mathrm{a}$, the z component of the electric field is

$$E_z = E_0 \left[3\frac{\sigma_0}{\sigma_z} - \frac{\sigma_0}{\sigma_z}\left(\frac{c}{b} + \frac{c}{a}\right)\right], \tag{7}$$

and the electric power is

$$\overline{P_\mathrm{a}} = \sigma_0 \overline{E_0^2} \left[2 + \frac{\sigma_0}{\sigma_z}\left(3 - 2\frac{c}{a}\right)^2 \right]. \tag{8}$$

The resistance is inversely related to the conductivity, $\sigma = \rho^{-1}$. The ratio of isotropic and anisotropic electric power may take the following form:

$$\frac{\overline{P_\mathrm{a}}}{\overline{P_\mathrm{i}}} = \frac{1}{3}\left[2 + \frac{\rho_z}{\rho_x}\left(3 - 2\frac{c}{a}\right)^2 \right], \tag{9}$$

which depends on the ratio of resistivity and the ratio of lattice length. In other words, the energy dissipation relies on the material properties. Let us discuss two special cases to study Eq. (9). The first case is that the components in the x and y axes equal to the component in the z axis, and the energy dissipation is the same ($\overline{P}_\mathrm{a} = \overline{P}_\mathrm{i}$). In other words, the energy dissipation of the anisotropic case returns to that of the isotropic case. The second case is based on the experimental parameters of Sn structure.[32] The lattice length of the z component is less than that of the x component $c < a$, but the resistivity of the x component is larger than that of z component $\rho_z > \rho_x$, it is proved that $\overline{P}_\mathrm{a} > \overline{P}_\mathrm{i}$. In the second case, the energy dissipation in the anisotropic structure is larger than that in the isotropic structure.

When the high current density passes through the single crystal metal, some grains will be rotated due to the electromigration.[33–35] The geometric parameters in the rotating anisotropic case still keep the same condition as in the anisotropic case, but the difference is the body has been rotated. θ is the angle between the y axis (or z axis) and y' axis (or z' axis), ϕ is the angle between the x axis and x' axis. Under this condition, the body is rotated from one coordinate to the other coordinate. The transformation matrix can be written as[36]

$$\boldsymbol{A}^\star = \begin{pmatrix} \cos\phi & \sin\phi & 0 \\ -\cos\theta\sin\phi & \cos\theta\cos\phi & \sin\theta \\ \sin\theta\sin\phi & -\sin\theta\cos\phi & \cos\theta \end{pmatrix} \boldsymbol{A}. \tag{10}$$

If $\boldsymbol{E}$ indicates the electric field before rotating and $\boldsymbol{E}^*$ denotes the electric field after rotating, their components are related to

$$\begin{aligned} E_x^\star &= (\cos\phi + \sin\phi)E_0, \\ E_y^\star &= -\cos\theta(\sin\phi - \cos\phi)E_0 + \sin\theta E_z, \\ E_z^\star &= \sin\theta(\sin\phi - \cos\phi)E_0 + \cos\theta E_z, \end{aligned} \tag{11}$$

the electric current for rotating grain is

$$\begin{aligned} I_\mathrm{a}^\star = {} & \sigma_x E_0[(\cos\phi + \sin\phi)bc + (-\cos\theta\sin\phi + \cos\theta\cos\phi)ac] \\ & + \sigma_z E_0 \sin\theta(\sin\phi - \cos\phi)ab \\ & + E_z a(\sigma_x c\sin\theta + \sigma_z b\cos\theta). \end{aligned} \tag{12}$$

When the electric current is constant, the z component of the electric field is given by

$$\begin{aligned} E_z = {} & \frac{E_0}{\left(\frac{c}{a}\sin\theta + \frac{\sigma_z}{\sigma_x}\cos\theta\right)} \left\{ 3 - \frac{c}{a}\left[(\cos\phi + \sin\phi)\right.\right. \\ & \left.\left. + (-\sin\phi + \cos\phi)\cos\theta\right] - \frac{\sigma_z}{\sigma_x}\sin\theta(\sin\phi - \cos\phi)\right\}. \end{aligned} \tag{13}$$

Through the complicated derivation, we obtain the following expressions about the ratio of $\overline{P_\mathrm{a}^\star}$ and $\overline{P_\mathrm{i}}$:

$$\begin{aligned} \frac{\overline{P_\mathrm{a}^\star}}{\overline{P_\mathrm{i}}} = {} & \frac{1}{3\left(\frac{c}{a}\sin\theta + \frac{\rho_x}{\rho_z}\cos\theta\right)^2} \left\{ (1 + \cos^2\theta + \sin(2\phi)\sin^2\theta) \right. \\ & \left. \times \left(\frac{c}{a}\sin\theta + \frac{\rho_x}{\rho_z}\cos\theta\right)^2 \right. \end{aligned}$$

$$
\begin{aligned}
&+(\sin^2\theta+\frac{\rho_x}{\rho_z}\cos^2\theta)\\
&\times\left[3-2\frac{c}{a}\left(\cos^2\frac{\theta}{2}\cos\phi+\sin^2\frac{\theta}{2}\sin\phi\right)\right]^2\\
&+\frac{\rho_x}{\rho_z}\sin^2\theta(1-\sin(2\phi))\\
&\times\left[\left(\frac{c}{a}\right)^2\sin^2\theta+\frac{c}{a}\sin(2\theta)+\frac{\rho_x}{\rho_z}(1+\cos^2\theta)\right]\\
&+\sin\theta(\cos\phi-\sin\phi)\left[\frac{c}{a}\left(1-\frac{\rho_x}{\rho_z}\right)\sin(2\theta)+2\frac{\rho_x}{\rho_z}\right]\\
&\times\left[3-2\frac{c}{a}\left(\cos^2\frac{\theta}{2}\cos\phi+\sin^2\frac{\theta}{2}\sin\phi\right)\right]\Big\}, \qquad (14)
\end{aligned}
$$

which depends on four kinds of factors: θ and ϕ the rotation properties, and ρ_x/ρ_z and c/a the anisotropic properties of materials. However, one can find that the rotation case can be returned to the non-rotation case $\overline{P_{\rm a}^{\star}}=\overline{P_{\rm a}}$ when θ and ϕ are taken as 0 respectively. We adopt the experimental parameters of β-Sn, the resistivity of z and x components is 20.27 Ω·cm and 13.25 Ω·cm, respectively, and the lattice constants are $l_x=l_y=0.583$ nm and $l_z=0.318$ nm, respectively. The energy dissipation with the experimental parameters of lattice constants and resistivity for β-Sn as a function of the angles along the longitudinal and transversal directions is depicted in Fig. 1. When $\phi=0$, the energy dissipation considerably increases in θ, indicating the increase of energy dissipation along the current direction. However, if the ϕ angle is also changed, the energy dissipation will become a multi-valued region. The ranges of θ and ϕ are from 0 to about 45, and from 0 to about 50, respectively. The energy dissipation has a slightly lower value, in the other range, the energy dissipation will have different strengths, which means that different anisotropic directions will cause different Joule heating. Therefore, these theoretical works are very useful and are able to guide the choice of different materials to protect the generation of Joule heating before people try to get good experimental results.

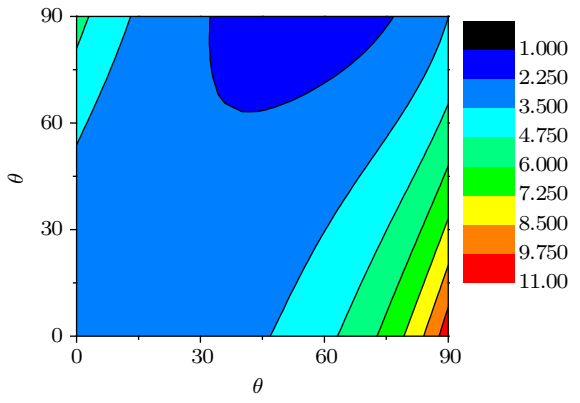


Fig. 1. (color online) The relationship between the energy dissipation and the angles along the longitudinal as well as transversal directions in the rotation β-Sn system, where the resistivity parameters are $\rho_x=\rho_y=13.25$ Ω·cm, and $\rho_z=20.27$ Ω·cm and the lattice parameters are $l_x=l_y=0.583$ nm, and $l_z=0.318$ nm.

3. Results and discussion

The energy dissipation is not the same in different orientations and different anisotropic materials, so we can choose materials to control the growth processes as well as the microstructure of materials. The effects of lattice and resistivity parameters on the energy dissipation are shown in Fig. 2, where the range of the ratio of lattice length is from 0 to 5 and the range of the ratio of resistivity is from 0 to 5, respectively. Based on this calculation, we find that the energy dissipation for different material parameters has a huge difference, the value of energy dissipation is from 0 to 90. We will give two examples to discuss the relationship between energy dissipation and orientations for different anisotropic materials.

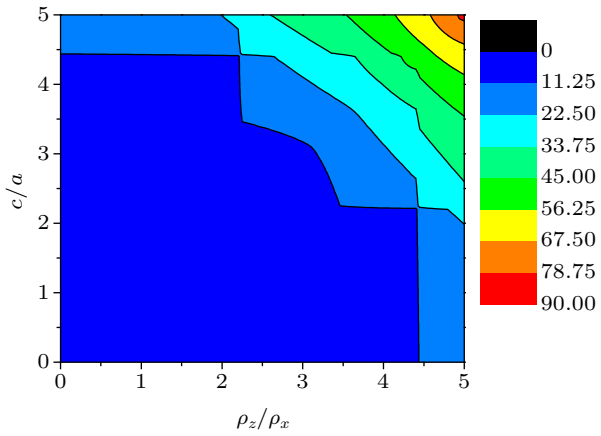


Fig. 2. (color online) Energy dissipation varies with the ratio of lattice lengths and the ratio of resistivity.

As the first example, the materials with the ratio of resistivity $\rho_x/\rho_z=0.5$ and the ratio of lattice length $c/a=0.5,1.5,2.5,5.0$ are chosen respectively, whose simulation results are shown in Fig. 3. The relationship between angles θ and ϕ is approximately the series of slope lines shown in Fig. 3(a), whose pattern formation is similar to a group of strip phases. The Joule heating has the lowest value in the second strip. The larger energy dissipation will occur in the larger θ and the lower ϕ range. The different pattern can be seen in Fig. 3(b), in which lower Joule heating is located in most ranges and larger Joule heating is in larger ϕ and lower θ range. For the condition of $\rho_x/\rho_z=0.5$, $c/a=2.5$, the relationship between the energy dissipation and orientation is plotted in Fig. 3(c), where the lower energy dissipation appears in most ranges; this case is different from the case shown in Fig. 3(b), where the larger energy dissipation will be in both larger and lower ϕ and lower θ ranges. The other interesting phenomena occur in Fig. 3(d), the energy dissipation is lower in almost all ranges, but the higher energy dissipation occurs in the lower θ and ϕ range.

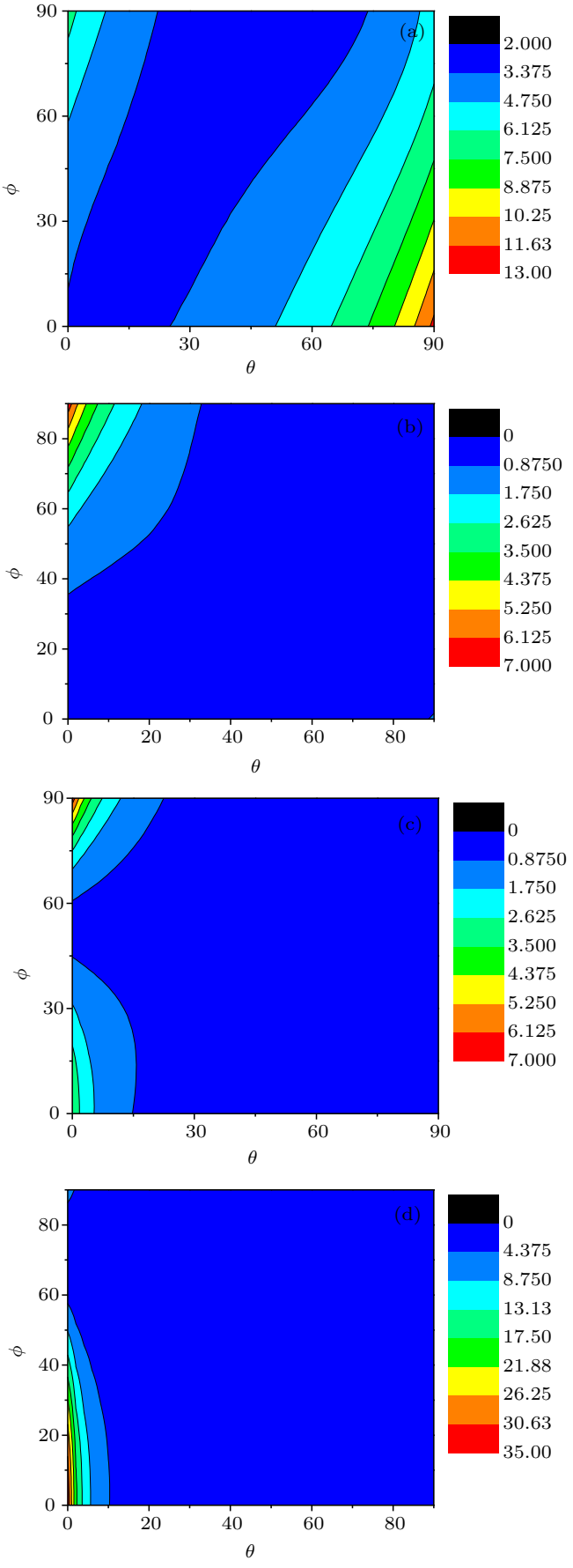


Fig. 3. (color online) Energy dissipation as a function of the angles along the longitudinal and transversal directions: (a) $\rho_x/\rho_z = 0.5$, $c/a = 0.5$, (b) $\rho_x/\rho_z = 0.5$, $c/a = 1.5$, (c) $\rho_x/\rho_z = 0.5$, $c/a = 2.5$, (d) $\rho_x/\rho_z = 0.5$, $c/a = 5.0$.

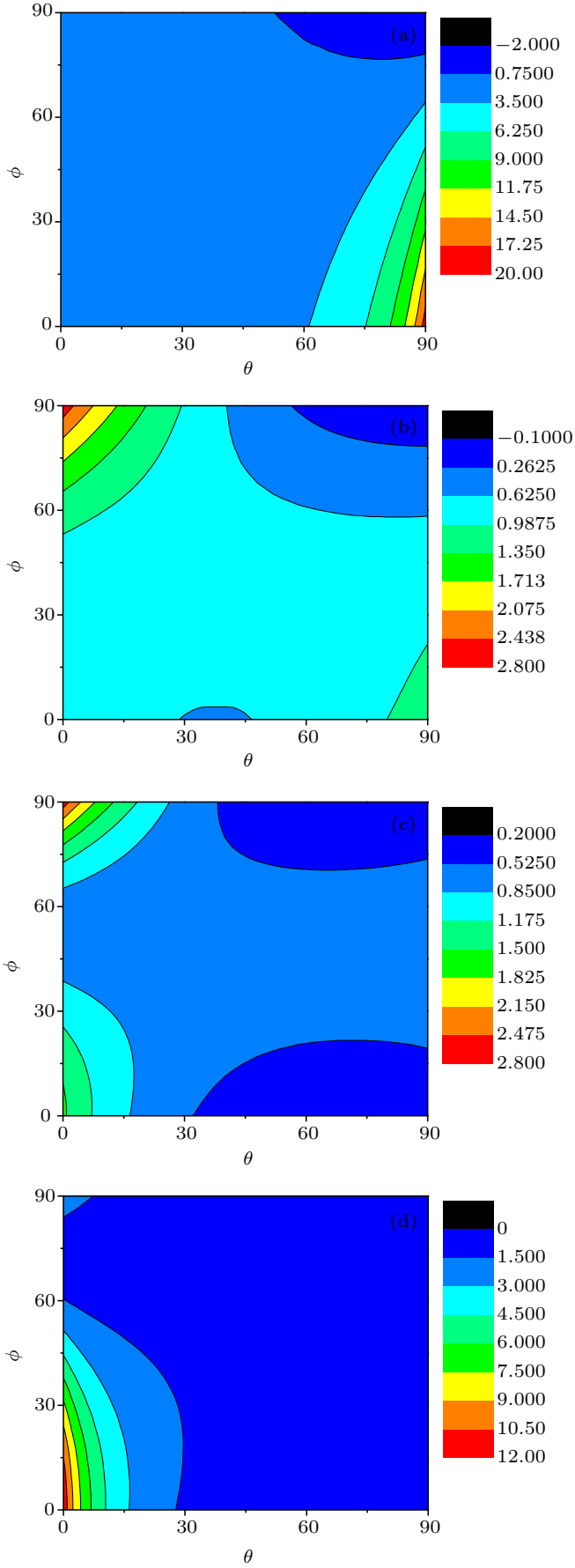


Fig. 4. (color online) The effect of energy dissipation with different material parameters: (a) $\rho_x/\rho_z = 1.5$, $c/a = 0.5$, (b) $\rho_x/\rho_z = 1.5$, $c/a = 1.5$, (c) $\rho_x/\rho_z = 1.5$, $c/a = 2.5$, and (d) $\rho_x/\rho_z = 1.5$, $c/a = 5.0$.

The second example is the material with the ratio of resistivity 1.5 and the ratio of lattice length $c/a = 0.5, 1.5, 2.5, 5.0$ respectively. The relationship between the energy dissipation and the angles along the longitudinal as well as transversal orientations is illustrated in Fig. 4. The middle strength of energy dissipation (from 0.75 to 3.5) is in most ranges as we can observe in Fig. 4(a) that the larger energy dissipation will occur in the larger θ and the lower ϕ. From Figs. 4(b) and 4(c), we can find that Joule heating is lower in all ranges (the maximal value is 2.8). However, as shown in Fig. 4(d), the largest Joule heating is approximately 12, which is much larger than that shown in Figs. 4(b) and 4(c). In terms of the above simulation, we can see that the material parameters with $\rho_x/\rho_z, c/a = 1.5$ or 2.5 have the lower energy dissipation. In other words, our models and calculations can be helpful for choosing a suitable anisotropic material.

The multigrain structures are an interesting and important subject in metallic physics[37] and nano-scale physics.[38–40] It is assumed that every grain is uniform and the same electric current, and θ_i is the angle between the horizontal direction and the electric current direction in the i-th grain. We assumed that ϕ angle is fixed as zero for every grain. This case likes a series circuit because grains are arranged in a chain, where the electric current for every grain is the same. Meanwhile, the condition of a constant electric current has been applied in the previous models; it is proved that the electric field for every grain can be calculated. Therefore, the total average electric power is the sum of the electric power for every grain. According to this idea, two specific cases will be discussed. The first is the multigrain with the repeatable configuration for two layers, which has two repeatable AB layers, i.e., the multilayer structures are ABAB$\cdots$AB; we called these multilayers the AB stack.[41,42] The second case is the sandwich structure, which only consists of three layers and forms an ABC stack.

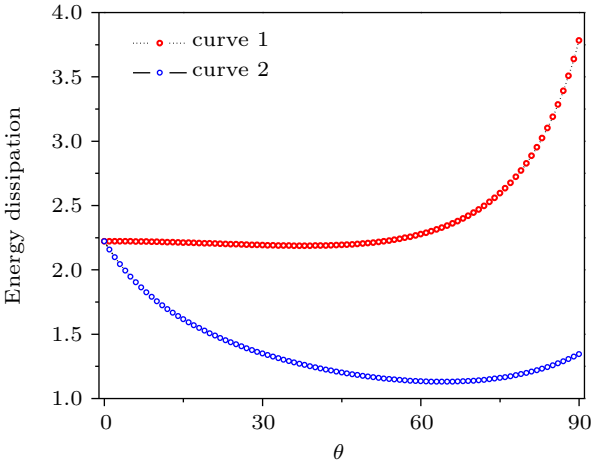


Fig. 5. (color online) The relationship between the energy dissipation and different orientation for repeatable two layers, where the parameters of the A layer are $\rho_x/\rho_z = 1.5$, $c/a = 2.5$ and the parameters of the B layer are $\rho_x/\rho_z = 2.5$, $c/a = 1.5$.

Figure 5 plots the relationship between the energy dissipation and the configuration of multigrain with repeatable two layers, where the parameters of the A layer are the length ratio $c/a = 1.5$ and resistivity ratio $(\rho_x/\rho_z = 2.5)$, while the B layer's are $(c/a = 2.5)$ and $(\rho_x/\rho_z = 1.5)$. The relationship between the energy dissipation and different orientations is a nonlinear function. Two curves have different trends, curve 1 is an increasing function with angle θ, curve 2 exists at a minimum value of energy dissipation located at about $\theta = 70°$. It is shown that the energy dissipation has different behaviors for different materials.

The multigrain can be reduced to the tri-layers: one layer with θ_1 configuration, the second layer with $\theta = 0$, the third layer with θ_2 orientation. We select the parameters for two sandwich structures, the first sandwich structure is the ABA structure that the parameters for the first A layer are chosen as $c^{\mathrm{A}}/a^{\mathrm{A}} = 1.5$ and $\rho_x^{\mathrm{A}}/\rho_z^{\mathrm{A}} = 2.5$, the second layer with $c^{\mathrm{B}}/a^{\mathrm{B}} = 1.5$ and $\rho_x^{\mathrm{B}}/\rho_z^{\mathrm{B}} = 1.5$, and the parameters of the third layer are the same as the first layer $c^{\mathrm{C}}/a^{\mathrm{C}} = 1.5$ and $\rho_x^{\mathrm{C}}/\rho_z^{\mathrm{C}} = 2.5$. Figure 6(a) shows that the relationship between θ_1 and θ_2 looks like a parabolic form. The energy dissipation decreases with the increase of angle θ_1. It is demonstrated that the energy dissipation depends on the angle θ_1; in other words, the energy dissipation is almost independent of θ_2. The parameters of the second

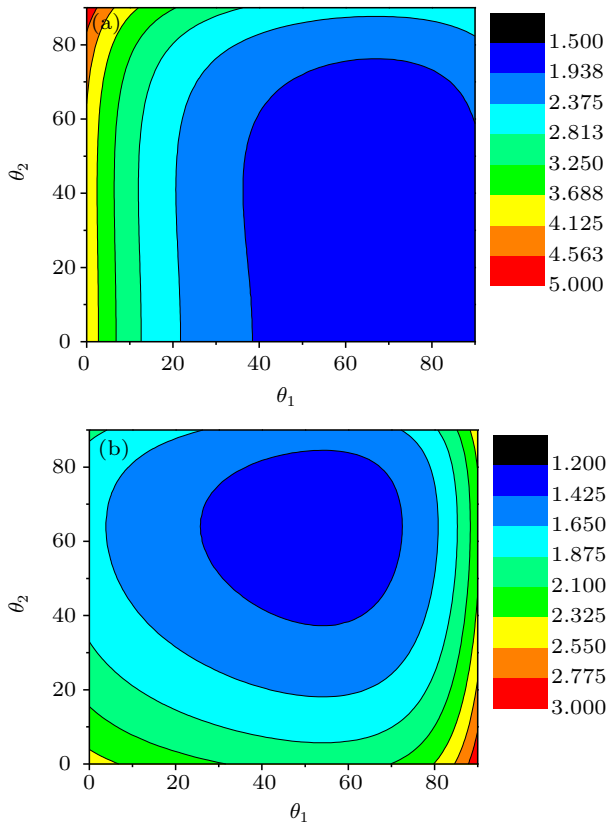


Fig. 6. (color online) Energy dissipation as a function of two different orientations θ_1 and θ_2. (a) The first sandwich structure ABA (A: $\rho_x/\rho_z = 2.5, c/a = 1.5$, B: $\rho_x/\rho_z = 1.5$, $c/a = 1.5$, C = A: $\rho_x/\rho_z = 2.5$, $c/a = 1.5$), (b) the second sandwich ABC structure (A: $\rho_x/\rho_z = 1.5$, $c/a = 2.5$; B: $\rho_x/\rho_z = 2.5$, $c/a = 2.5$; C: $\rho_x/\rho_z = 2.5$, $c/a = 1.5$).

sandwich structures ABC are chosen as the first A layer with $c^{\mathrm{A}}/a^{\mathrm{A}} = 1.5$ and $\rho_x^{\mathrm{A}}/\rho_z^{\mathrm{A}} = 2.5$, the second layer with $c^{\mathrm{B}}/a^{\mathrm{B}} = 2.5$ and $\rho_x^{\mathrm{B}}/\rho_z^{\mathrm{B}} = 2.5$, the third layer with $c^{\mathrm{C}}/a^{\mathrm{C}} = 2.5$ and $\rho_x^{\mathrm{C}}/\rho_z^{\mathrm{C}} = 1.5$. Figure 6(b) is very different from Fig. 6(a). The relationship between θ_1 and θ_2 looks like a concentric circle, thus the energy dissipation depends on both θ_1 and θ_2. The energy dissipation in the center circle has the minimum value. Larger rotation of grain leads to larger Joule heating, which implies the importance of rotating properties for the microstructural evolution under electromigration. It can be seen that the configuration dependence of energy dissipation varies.

4. Conclusion

We present models and calculations to describe the energy dissipation of anisotropic materials. The expression of the energy dissipation in the anisotropic system in the case of constant current can be derived from the first principles. It is shown to depend on the lattice parameters and resistivity. We obtain the relationship between energy dissipation and the angles along the longitudinal and transversal directions. It is shown that the orientation variation of grain can significantly influence the energy dissipation for some anisotropic materials. On the other hand, two multigrain models are constructed. It is demonstrated that the microstructural evolution under electromigration can be radically influenced by the energy dissipation and the anisotropic configuration.

References

[1] Tu K N 2003 *J. Appl. Phys.* **94** 5451
[2] Blech I A and Sello H 1967 *Physics of Failure in Electronics* **5** 496
[3] Lu M, Shih D Y, Lauro P, Goldsmith C and Henderson D W 2008 *Appl. Phys. Lett.* **92** 211909
[4] Huntington H B and Grone A R 1961 *J. Phys. Chem. Solids* **20** 76
[5] Rosenberg R, Edelstein D C, Hu C K and Rodbell K P 2000 *Annu. Rev. Mater. Sci.* **30** 229
[6] Tu K N 1994 *IBM Tech. Discl. Bull.* **37** 61
[7] Landauer R and Woo J W F 1974 *Phys. Rev. B* **10** 1266
[8] Zhang L Y, Ou S Q, Huang J, Tu K N, Gee S and Nguyen L 2006 *Appl. Phys. Lett.* **88** 012106
[9] Lee T Y, Tu K N and Frear D R 2001 *J. Appl. Phys.* **90** 4502
[10] Yeh E C C, Choi W J, Tu K N, Elenius P and Balkan H 2002 *Appl. Phys. Lett.* **80** 580
[11] Yan H, Zhang W J, Jiang H Y and Chen L 2014 *Chin. Phys. B* **23** 040702
[12] Liu C Y, Chen C and Tu K N 2000 *J. Appl. Phys.* **88** 5703
[13] Tu K N and Gosele U 2005 *Appl. Phys. Lett.* **86** 093111
[14] Zhang L, Ma G J, Lin G Q, Ma H and Han K C 2014 *Chin. Phys. B* **23** 048102
[15] Lang N D and Avouris P 1998 *Phys. Rev. Lett.* **81** 3515
[16] Tang Z K, Zhang L Y, Wang N, Zhang X X, Wen G H, Li G D, Wang J N, Chan C T and Sheng P 2001 *Science* **292** 2462
[17] Cao Y Z, Li G J, Wang Q, Ma Y H, Wang H M and He J C 2013 *Acta Phys. Sin.* **62** 227501 (in Chinese)
[18] Yin Y D, Rioux R M, Erdonmez C K, Hughes S, Somorjai G A and Alivisatos A P 2004 *Science* **304** 711
[19] Todorov T N, Hoekstra J and Sutto A P 2001 *Phys. Rev. Lett.* **86** 3606
[20] Ventra M D and Chen Y C 2004 *Phys. Rev. Lett.* **92** 176803
[21] Wei B Q, Vajtai R and Ajaya P M 2001 *Appl. Phys. Lett.* **79** 1172
[22] Ho P S and Kwok T 1989 *Rep. Prog. Phys.* **52** 301
[23] Blech I A and Meieran E S 1967 *Appl. Phys. Lett.* **11** 263
[24] Dekker J P, Volkert C A, Arzt E and Gumbsch P 2001 *Phys. Rev. Lett.* **87** 035901
[25] Todorov T N 2001 *J. Phys. Condens. Matter* **13** 10125
[26] Spolenak R, Kraft O and Arz E 1998 *Microelectron. Reliab.* **38** 1015
[27] Kunz M, Tamura N, Chen K, MacDowell A A, Celestre R S, Church M M, Fakra S, Domning E E, Glossinger J M, Plate D W, Smith B V, Warwick T, Padmore H A and Ustundag E 2009 *Review of Scientific Instruments* **80** 035108
[28] Callister W D Jr 2000 *Materials Science and Engineering an Introduction* (New York: Wiley)
[29] Wu A T, Tu K N, Lloyd J R, Tamura N, Valek B C and Kao C R 2004 *Appl. Phys. Lett.* **85** 2490
[30] Nye J F 1985 *Physical Properties of Crystals: Their Representation by Tensors and Matrices* (New York: Oxford University Press)
[31] Stratton J A 1941 *Electromagnetic Theory* (New York: McGraw-Hill)
[32] Bridgman P W 1952 *Proc. Am. Acad. Arts. Sci.* **81** 167
[33] Chen K, Tamura N and Tu K N 2009 *Materials Research Society Symposium Proceedings* **I05-06** 1116
[34] Lloyad J R 2003 *J. Appl. Phys.* **94** 6483
[35] Chen K, Tamura N, Kunz M, Tu K N and Lai Y S 2009 *J. Appl. Phys.* **106** 023502
[36] Goldstein H 1950 *Classical Mechanics*
[37] Tu K N 1977 *J. Appl. Phys.* **48** 3400
[38] Parkin S S P, More N and Roche Y P 1990 *Phys. Rev. Lett.* **64** 2304
[39] Steren L B, Barthelemy A, Duvail J L, Fert A, Morel R and Petroff F 1995 *Phys. Rev. B* **51** 292
[40] Zhang L Y, Sun H, Li B Z and Pu F C 1999 *J. Phys. D: Appl. Phys.* **32** 1214
[41] Zhang S and Levy P M 1996 *Phys. Rev. Lett.* **77** 916
[42] Itoh H, Inoue J and Maekawe S 1996 *Phys. Rev. Lett.* **77** 916